

A molecular dynamics simulation of water confined in a cylindrical SiO_2 pore.

M. Rovere*, M.A. Ricci, D. Vellati and F. Bruni
Dipartimento di Fisica, Università di Roma Tre
Via della Vasca Navale 84, 00146 Roma, Italy.
INFN, Unità di Ricerca Roma Tre

A molecular dynamics simulation of water confined in a silica pore is performed in order to compare it with recent experimental results on water confined in porous Vycor glass at room temperature. A cylindrical pore of 40\AA is created inside a vitreous SiO_2 cell, obtained by computer simulation. The resulting cavity offers to water a rough hydrophilic surface and its geometry and size are similar to those of a typical pore in porous Vycor glass. The site-site distribution functions of water inside the pore are evaluated and compared with bulk water results. We find that the modifications of the site-site distribution functions, induced by confinement, are in qualitative agreement with the recent neutron diffraction experiment, confirming that the disturbance to the microscopic structure of water mainly concerns orientational arrangement of neighbouring molecules. A layer analysis of MD results indicates that, while the geometrical constraint gives an almost constant density profile up to the layers closest to the interface, with a uniform average number of hydrogen bonds (HB), the hydrophilic interaction produces the wetting of the pore surface at the expenses of the adjacent water layers. Moreover the orientational disorder together with a reduction of the average number of HB persists in the layers close to the interface, while water molecules cluster in the middle of the pore at a density and with a coordination similar to bulk water.

61.20.Ja, 61.20.-p, 61.25.-f

*Author to whom correspondence should be addressed

I. INTRODUCTION

Recent literature reports on many studies about the structural and dynamical properties of water confined in different environments.¹ The interest on this subject arises mainly from evidence of the relevance of the water-substrate interaction in determining either stability and enzymatic activity of proteins or swelling of clay minerals. In this respect it is also important to elucidate to what extent water itself is significantly perturbed from its bulk behavior, when confined within a porous material, and in particular how far from the interface does the perturbation propagate through the liquid and whether it depends on the nature of the interaction (hydrophilic or hydrophobic).

All the experimental studies of the dynamics of water molecules confined in different substrates agree in suggesting a slowing down of the translational single molecule motion¹⁻³ compared to the bulk liquid phase, while the same kind of agreement is not found in the interpretation of structural data.⁴⁻⁹ Most neutron diffraction studies are indeed interpreted in terms of more extensive hydrogen bonding than in bulk water, at least in the water layers closer to the interface and below room temperature⁴⁻⁷, contrarily to what found in a recent study performed by some of us.^{8,9} As a matter of fact this study differs from previous ones in two relevant aspects: first, only in this case hydrogen/deuterium substitution in the neutron diffraction experiment was exploited, thus allowing the estimate of three site-site radial distribution functions; second, full account of the excluded volume effects on the radial distribution functions was attempted for the first time. Although the limitations of the experimental technique do not allow to draw definitive and quantitative conclusions, nevertheless it was apparent from this study that water confined in porous Vycor glass is still hydrogen bonded, but the bond network is strongly distorted even at room temperature. The above mentioned experimental limitations are due to the presence of contributions to the measured cross section due to the cross correlations between water atoms and Vycor atoms, which cannot be isolated from the water-water correlations in the neutron diffraction experiment. As a consequence in the experiment only three composite site-site distribution functions are accessible through the isotopic substitution, namely $g_{HH}(r)$, $g_{XH}(r)$, and $g_{XX}(r)$, where the subscript H stays for all hydrogen atoms in the sample (either water hydrogens or protons bonded to the pore surface) and X labels all non substituted atoms (i.e. water oxygens or Vycor atoms).^{8,9} Information about the relative arrangement of water atoms may then be masked by the cross correlation terms: to extract this information from the experiment the hypothesis that the microscopic structure of confined water does not change upon changing the hydration state was proposed.⁹ Molecular Dynamics (MD) simulations on the contrary do not suffer from such limitations, as individual atomic species may be labelled and the corresponding distribution functions calculated, thus providing an useful test of the entire data analysis procedure.

To our knowledge, only a few MD studies on the modifications of water structure and/or dynamics in the presence of a substrate interaction have been so far performed¹⁰⁻¹⁴, for both hydrophobic or hydrophilic interactions. All these studies indicate that water perturbations are both short ranged and relatively mild in magnitude. However the investigated geometries may hardly be comparable with the extended and fractal-like network of thin cylindrical pores offered by Vycor glass. Since the nature of the substrate-water interaction along with the geometrical characteristics of the confinement may influence the structure of interstitial water¹⁵, we present here a MD simulation of TIP4P water, confined in a cylindrical pore built inside a SiO₂ glass.

II. MOLECULAR DYNAMICS OF WATER IN A SILICA CAVITY

To model the cylindrical cavity of a porous glass, like Corning Vycor glass¹⁶, we follow the method proposed by Brodka and Zerda¹⁷ in the simulation of liquid acetone in silica pores. A vitreous silica (SiO_2) of 192 atoms is obtained by performing a MD simulation with the empirical potential model of Feuston and Garofolini.¹⁸ Starting from a cristobalite crystalline structure¹⁹, the system is melted at $6000K$ and then quenched to room temperature with the method described in Ref. 20 and 17. Since we need a cylindrical cavity of 40\AA of diameter, which corresponds to the average size of the Vycor glass pores, the small glass cell is repeated five times along the three directions in order to get a cubic cell of approximately 19000 atoms with a box length of $L = 70\text{\AA}$. We create a cavity inside the glass by removing the atoms lying within a distance $R = 20\text{\AA}$ from the z -axis. Then we remove from the cavity surface also the silicon atoms bonded to less than four oxygens. This procedure leaves on the pore surface a number of *non bridging* oxygens (nbO), i.e. oxygen atoms bonded to only one silicon, and is a reasonable replica of the industrial preparation of the sample.¹⁶ Surface oxygens bonded to two silicon atoms will be in the following referred to as *bridging* oxygens (bO). This nomenclature is in agreement with previous literature.¹⁷ Since in the experiment the nbO were saturated with protons prior to hydration, we attach extra hydrogen atoms to the nbO found on our simulation cell surface. The surface hydrogens are placed at the equilibrium distance (0.95\AA) from a nbO with a Si-O-H angle of 116° . We notice that the procedure described above generates a cavity with a rough surface, with geometry and size similar to the average ones in the real porous Vycor glass. The actual volume of the cavity, V_p , generated inside our simulation box is indeed unknown and only roughly approximated to a lower value by the volume of a cylinder of radius $R = 20\text{\AA}$.

In the simulation we use the model TIP4P²¹ for water. Water molecules interact with the substrate atoms with a potential modeled according to Ref. 17, where different Lennard-Jones (LJ) parameters and fractional charges are assumed for bO and nbO. Silicon and surface hydrogen atoms interact only via coulombic forces with the charged water sites. LJ parameters and fractional charges for the SiO_2 sites and TIP4P water are given in Table 1. The cross LJ parameters are calculated with the usual Lorentz-Berthelot rules. During the simulation the substrate atoms and the surface hydrogens do not move. Periodic boundary conditions are applied only along the axis of the cylinder (z -direction). All the pair interactions are truncated at a cutoff radius of $r_c = 9\text{\AA}$ and reaction field corrections are applied.^{22,23}

The number of particles to use is determined by the density of the confined water at full hydration in the neutron diffraction experiment²⁴, i.e. $n = 0.0297\text{\AA}^{-3}$ corresponding to $N = 2661$ molecules. The simulation starts with the centers of the molecules placed in a fcc lattice, where the occupied nodes are randomly chosen. The size of the lattice is such that it is contained in the cylindrical pore. The origin of the coordinates is assumed in the middle of the cylinder axis. The initial velocities are chosen randomly with a distribution consistent with the required temperature. The equation of motions are solved with the popular quaternion-leapfrog algorithm due to Fincham.²² Confined water is melted at $500K$ and then equilibrated at $300K$. Initially a very small time step of $10^{-4}ps$ is used then it is slowly increased. We find that for time steps larger than $5 \times 10^{-3}ps$ we need a too frequent rescaling of the temperature, so the final runs are done with a time step of $10^{-3}ps$. The calculation of the forces during the simulation is performed with a neighbour list built by using a cell method²⁵, thus allowing the simulation to be run on an Alpha station.

III. SITE-SITE DISTRIBUTION FUNCTIONS

The calculation of the site-site radial distribution functions of confined water is motivated by the possibility of comparing with the experimental results recently obtained with the use of the isotopic substitution technique in neutron diffraction experiments.^{8,9} On the other hand the site-site distribution functions can be easily calculated from computer simulation, when periodic boundary conditions are applied in all three directions, but in our case, where the system is confined in a cylindrical box one must carefully take care of the excluded volume effects, as discussed recently by Ref. 15 and 9. As a matter of fact the radial distribution functions obtained either experimentally or by simulation for a confined liquid cannot readily compare with those of the corresponding bulk, due to the existence of regions, where the liquid is not allowed. In this case indeed the radial distribution function of a system of non interacting particles, the so called *uniform fluid*, is not equal to unity at all r values, but approaches its asymptotic value with a profile which depends on the size and shape of the confining volume. As a consequence the site-site distribution functions of the interacting liquid, which are defined with respect to that of the uniform fluid, do not lay on a flat profile and the amplitude of their oscillations may also show a trivial r -dependence.^{15,26}

Our MD results could directly compare with the experimental data of Ref. 9 only if the simulation box was topologically identical to the real Vycor glass sample and if the site-site distribution functions of TIP4P water were correctly reproducing those of real bulk water. Since both conditions are only approximately matched, we will perform the corrections for the excluded volume effects on our MD calculated site-site distribution functions, to compare the corrected ones with those of TIP4P bulk water. The aim of this comparison will be to test whether we observe the same qualitative modifications with respect to bulk water observed in ref. 9.

From the configurations obtained in the molecular dynamics simulation one can calculate for each site of type α , placed in the origin of the reference frame, the number of sites of type β lying inside a spherical shell $\delta v(r)$ of thickness δr at distance r from the origin and obtain the average number of site pairs $\bar{n}_{\alpha\beta}^{(2)}(r)$. Following the usual recipes²², regardless of the confinement inside an almost cylindrical volume, the computer simulated distribution function is then calculated as

$$g_{\alpha\beta}^{MD}(r) = \frac{\bar{n}_{\alpha\beta}^{(2)}(r)}{\frac{N_\beta}{V_p} \delta v(r)} \quad (1)$$

where N_β is the number of β sites. The results obtained for the $g_{\alpha\beta}^{MD}(r)$ functions are shown in Figs. 1a - 1c. They are compared with the same functions obtained in a simulation, where water is purely confined in the cylindrical pore without any interaction with the substrate atoms. The large difference between the intensity of the first peaks of the two oxygen-oxygen $g_{OO}^{MD}(r)$ functions indicates that switching on the interaction with the substrate atoms is equivalent to enhance the confinement effects. The same trend is observed for the other functions and particularly in the oxygen-hydrogen $g_{OH}^{MD}(r)$ one, where the so called hydrogen bond peak at $r \approx 1.85\text{\AA}$ is strongly enhanced. However, as we will see below, this is not an evidence of an increase of the number of hydrogen bonds in the confined system, but a trivial effect of the geometrical confinement.²⁶

From the Figs. 1a - 1c it is clear that in the limit of large r all three site-site correlation functions of confined water go below the exact limit of unity. This is a finite size effect due to the absence of periodic boundary conditions along the x and y directions.

As already stated the site-site correlation functions (1) calculated in the computer simulation represent the fluctuations of the density with respect to a *uniform* density profile, which is not a constant as in non confined systems. Thus to obtain the corrected site-site distribution functions of water inside the pore $g_{\alpha w \beta w}(r)$ to be compared with those of the corresponding bulk liquid, we calculate, following Ref. 15 and 9:

$$g_{\alpha w \beta w}(r) = \frac{g_{\alpha \beta}^{MD}(r)}{g_u^{ww}(r)} \quad (2)$$

where $g_u^{ww}(r)$ is the *pair correlation function* of the confined uniform fluid.

At variance with the experiment, in the present computer simulation, water is confined in a single pore, thus neglecting the correlation between water molecules residing in different pores, nevertheless the molecular dynamics results can be corrected using the same basic results of Ref. 15 and 9. In particular the function $g_u^{ww}(r)$ can be obtained from the Fourier transform of the form factor of a cylinder.²⁷ Moreover to evaluate eq. (2) one has to take into account that the function $g_{\alpha \beta}^{MD}(r)$ is not known behind r_c and its asymptotic behaviour is not reliable, a problem already considered in the experiment where the $q \rightarrow 0$ limit of the structure factors are not available.⁹

Before commenting the MD results after correction for excluded volume effects, and comparing these with bulk water results, it is useful to remind the qualitative differences between bulk and confined water evidenced in Ref. 9. The water-water distribution function for the oxygen atoms of confined water $g_{OwOw}(r)$ has the first peak at 2.8\AA as in the bulk, although sharper and less intense, while the second peak is shifted towards 3.4\AA . Only minor differences are apparent in the distribution function of water oxygens and water+Vycor hydrogens, $g_{OwHw+s}(r)$, with respect to the $g_{OH}(r)$ of bulk water. In particular the H-bond peak has almost the same intensity in both liquids, although in the confined case it is sharper, and some excess intensity is visible between the two main peaks. The hydrogen-hydrogen distribution function of water sites, $g_{HwHw}(r)$, shows on the contrary a dramatic increase of the first peak at 2.3\AA , while the second one is almost completely washed out. All these results suggest that confined water is still H-bonded, nevertheless the orientational correlations between neighbouring water molecules are strongly influenced by the confinement, resulting in a highly distorted network of bonds. As far as the water-Vycor cross distribution functions are concerned, only the distribution functions of water oxygens and Vycor atoms (regardless of any distinction between oxygen and silicon), $g_{OwXs}(r)$, and that of Vycor atoms and water hydrogens, $g_{XsHw}(r)$, were extracted from the experiment. The first one shows an intense peak at 2.8\AA , followed by a second peak at 4.5\AA ; the second one shows modulations, with very low intensity at 2\AA and 3.4\AA .

In Fig. 2a - 2c we show the results obtained with a procedure similar to the one adopted in Ref. 9, in order to perform the corrections for the excluded volume effects. Due to the approximations involved in the derivation, our functions are not reliable below the minimum approach distances, evidenced in Fig. 2a - 2c by the arrows. The site-site correlation functions of the bulk TIP4P water at the density $n = 0.0297\text{\AA}^{-3}$ are also shown in the same figures: although this density does not correspond to a physical state for bulk water at ambient conditions, nevertheless we prefer this state as a reference, to avoid confusion of density effects with those due to confinement.

The oxygen-oxygen site-site distribution function (Fig. 2a) shows a first peak, which is lower in amplitude and sharper than in bulk water, in agreement with the experiment. Moreover there is an evident increase of intensity in the region between $3 - 4\text{\AA}$: an indication of a distortion of the hydrogen bond network found also in the

experiment.⁹ As far as the $g_{OwHw}(r)$ function is concerned, we notice a dramatic change of the amplitude of the second peak and of the first minimum, in comparison with bulk water, while only minor modifications of the H-bond peak seem to occur. This results suggest that while the average number of H-bonds, as measured by the integral under the first peak, does not sensibly change, the orientational order of neighbouring water molecules is strongly distorted in the confined geometry. The comparison with the experiment is not straightforward in this case, since neutrons cannot distinguish between water protons and protons bonded to nbO. Nevertheless we notice that also the experimental data do not evidence enhancements of the amplitude of the H-bond peak and that the disagreement found with our simulation as far as the amplitude of the second peak is concerned may, at least partly, be due to the protons on the cavity surface, contributing with a broad peak between 2 and 4 Å (see Fig. 3a). Moreover in Fig. 2b we notice that the peak around 7 Å, i.e. where the surface hydrogen contribution is already very low according to Fig. 3a, is in agreement with the experimental results.

The $g_{HwHw}(r)$ function (Fig. 2c) confirms the strong distortion of the orientational order, since the amplitudes of both first and second peaks decrease and the first minimum shifts towards lower r values. On the other hand this is the distribution function with the worst agreement with the experiment. Such disagreement may be ascribed to the potential model or to the approximation made in Ref. 9 to extract the water-water contribution from the measured structure factors (i.e. weak dependence on the hydration state).

The site-site distribution functions of the substrate atoms with respect to the water atoms can be obtained along the same procedure described for the $g_{\alpha w \beta w}(r)$ using eq. (2), with the appropriate substrate-water uniform fluid function $g_u^{sw}(r)$. Since the substrate atoms are confined in a region between the cylinder surface and the surface of the total simulation cell of length L , we assume that $g_u^{sw}(r)$ is the Fourier transform of the difference between the form factor of the cylinder of diameter L and the form factor of the internal cylinder with the diameter $2R = 40$ Å. In Fig. 3b we show the results for g_{OsOw} and g_{OsHw} . The behaviour of this functions agrees with the experiment, particularly the positions of the first peak in both functions are located close to the experimental results.

In conclusion our simulation agrees with the experiment at a qualitative level: both techniques suggest indeed that the H-bond network is strongly distorted in confined water, although this does not necessarily imply strong enhancement or depression of the H-bond peak.

IV. LAYER ANALYSIS OF THE MICROSCOPIC STRUCTURE

In order to gain a better insight into the microscopic structure of the confined water, we perform a careful analysis of the configurations obtained in molecular dynamics. We divide the cylindrical pore in ten concentric radial shells, the n^{th} shell being defined by

$$(n-1)\Delta R < \sqrt{(x^2 + y^2)} < n\Delta R \quad n = 1, \dots, 10 \quad (3)$$

where $\Delta R = R/10$. First of all we look at the average density in each shell.

From Fig. 4 we see that the density profile is not constant along the $r = \sqrt{(x^2 + y^2)}$ coordinate, and that it takes a value similar to that of bulk water at ambient conditions in the first layer, i.e. the one closer to the center of the cylinder. The density slowly decreases going towards the cylinder surface and abruptly increases at layer n. 9, close to the substrate surface. The last layer (n. 10) is in the volume excluded by the LJ repulsion. It is interesting to compare this result with

the calculation performed with the substrate-water interaction switched off. In this latter case the density is essentially constant up to layer n. 8 and decreases in the last two layers. The effect of the interaction is thus to attract few water molecules, mainly from layers 7 and 8, to the surface, as shown by the density increase at layer n.9. The disturbance, brought into the density profile by the presence of an interacting surface, seems to extend up to no more than 8\AA from the surface itself. Moreover we notice that the potential model used here, gives a modest hydrophilic effect, in comparison with Ref. 11; this may also depend on the geometrical symmetry of the interface, as already apparent from Ref. 13. At all layers, except the 10-th, the density is higher than its average value of $n = 0.0297\text{\AA}^{-3}$, due to the size of the LJ diameters. This qualitatively explains why experimentally one finds for confined water a lower average density than for bulk water.²⁴ On the other hand this finding needs a deeper investigation, because it may be dependent on both the potential model and the simulation technique adopted. In particular one should investigate whether in a NVE simulation the system tries to build up a kind of bulk phase at contact with the confined phase, due to the simultaneous constraints of a constant number of particles and a constant volume. Different computer simulation methods, where one allows the system to change density during the simulation²², could help to clarify this point.

In Fig. 5 we report the average number of HB in each shell (solid line), as calculated according to a geometrical definition.²⁸ We consider two water molecules as being hydrogen bonded if their O-O separation is less than 3.0\AA , their closest O-H separation is less than 2.3\AA and the $H - O \cdots O$ angle γ is less than 30° . As seen from Fig. 5 the number of HB almost monotonically decreases approaching the interface; in particular in the layer n. 9, where the density is highest, the number of HB goes below its density-weighted average value (dotted line in the figure). When the substrate-water interaction is turned off the number of HB is essentially constant up to the 9-th layer and decreases, as also the density does, in the last two layers. The comparison of the two profiles in Fig. 5 reveals that the pure geometrical confinement is responsible for the reduction of the number of HB at the interface; switching on the interaction does not sensibly modify this number, although the density at layer n.9 increases. Conversely, in the layers closer to the center of the pore, where the density reaches that of ambient water, even the number of HB approaches the values typical of bulk water at ambient conditions. The reduction of the number of HB in the intermediate layers seems also to be a density effect. Figs. 6a and 6b report the distributions of HB and the distribution of $\cos(\gamma)$ respectively. The histograms of Fig. 6a broaden and shift towards zero, approaching the pore surface, and also the distribution of $\cos(\gamma)$ markedly broadens for layer 9, compared with layers 1 and 5. The pattern of HB in the 9-th layer is severely disordered due to the orientational constraints, brought by the presence of a confinement. We notice that the results found for the internal layers cannot be distinguished from those for the bulk and the disturbance brought by the confinement in an interacting substrate extends up to 8\AA from the interface.

We have also calculated the number of HB between the water molecules, located in layers 9 and 10, and the hydrogens and oxygen atoms belonging to the cavity surface. This analysis, although biased by the low statistics, indicates that the number of such bonds is very low in the present simulation.

V. CONCLUSIONS

The results obtained by MD simulation of TIP4P water confined in a cylindrical SiO_2 pore have been compared with those of the simulation of the same liquid

after switching off the interaction with the substrate atoms and with those of the corresponding bulk liquid.

The first comparison indicates that the absence of periodic boundary conditions and the cylindrical symmetry of the confining volume are by themselves able to induce a significant distortion of the orientational order of water molecules, although leaving the density profile almost flat behind the shell closest to the interface. Indeed switching on the interaction with the substrate produces only an enhancement of the modulations of the distribution functions at short distances, without emergence of any new feature. Moreover when the interaction with the substrate is switched on, the competition between water-water and water-substrate interaction produces a minimum in the density profile at intermediate distances from the cavity surface on one side and the condensation of a *water drop* in the middle of the pore. This effect, although quite reasonable, may depend on the model and on the simulation technique and, as already stated, deserves a deeper investigation.

The observed phenomenon is accompanied by the occurrence of a dishomogeneous distribution of the H-bonds throughout the pore. While the water drop in the middle of the pore seems to have almost the same distribution of H-bonds as its bulk liquid, the average number of bonds decreases going towards the interface and its distribution becomes broader. It is noticeable that even in the shell closest to the interface, when the density reaches its maximum value, the average number of H-bonds is much lower than everywhere else. This suggests that the main effect of the confinement is to disturb the orientational arrangement of molecules to such an extent that a continuous network of bonds is not favoured up to distances from the interface of the order of 8\AA approximately.

As far as the intermolecular structure of water is concerned, the site-site distribution functions give only an average picture of the system. For this reason the H-bond peak of the $g_{OwHw}(r)$ function is not dramatically different from that of bulk TIP4P water, nevertheless it is clearly apparent from the comparison of all the three site-site distribution functions in Fig. 2 with their counterpart for the bulk liquid that the H-bond network is strongly distorted and that a number of interstitial (i.e. non H-bonded) neighbouring molecules must be present. This result is in qualitative agreement with the experimental findings of Ref. 9, although the distortion of the H-H correlation in that case seems more dramatic. However we must bear in mind that on one side MD results are model dependent and on the other side the experimental results were obtained assuming a weak hydration dependence of the partial structure factors, an hypothesis which deserves confirmation. As a matter of fact this MD study will continue to understand how the water structure depends on the hydration level.

A further comment on the potential model is mandatory. This model for the water-substrate interaction seems to be weakly hydrophilic. As a matter of fact the density in the water layer closest to the substrate increases only by the 10%. This may be due to the balance between the LJ repulsive interaction and the coulombic forces, as suggested also by the low number of bonds between water oxygens and protons bonded to nbO.

¹ S. H. Chen, and M. C. Bellissent-Funel, "Hydrogen Bond Networks", edited by M. C. Bellissent-Funel and J. C. Dore, NATO ASI Series C: Mathematical and Physical Science, **435**, 337 (Kluwer Academic Publishers, 1994).

- ² C. F. Polzanek and R. G. Bryant, J. Chem. Phys. **81**, 4038 (1984) B. P. Hills, and G. le Floc’k, Mol. Phys. **82**, 751 (1994).
- ³ M. C. Bellissent-Funel, and S. H. Chen, J. M. Zanotti Phys. Rev. **E51**, 4558 (1995).
- ⁴ D. C. Steytler, and J. C. Dore, Mol. Phys. **56**, 1001 (1985).
- ⁵ M. C. Bellissent-Funel, J. Lal, and L. Bosio, J. Chem. Phys. **98**, 4246 (1993).
- ⁶ D. C. Steytler, J. C. Dore, and C. J. Wright, Mol. Phys. **48**, 1031 (1983).
- ⁷ M. C. Bellissent-Funel, R. Sridi-Dorbez, and L. Bosio, J. Chem. Phys. **104**, 10023 (1996).
- ⁸ F. Bruni, M. A. Ricci, and A. K. Soper, submitted to J. Chem. Phys.
- ⁹ A. K. Soper, F. Bruni, and M. A. Ricci, submitted to J. Chem. Phys.
- ¹⁰ S. H. Lee, J. A. Mc Cammon, and P. J. Rossky, J. Chem. Phys. **80**, 4448 (1984).
- ¹¹ S. H. Lee, and P. J. Rossky, J. Chem. Phys. **100**, 3334 (1994).
- ¹² P. J. Rossky, "Hydrogen Bond Networks", edited by M. C. Bellissent-Funel and J. C. Dore, NATO ASI Series C: Mathematical and Physical Science, **435**, 337 (Kluwer Academic Publishers, 1994), and references therein.
- ¹³ L. Zhang, H. T. Davis, D. M. Kroll, and H. S. White, J. Phys. Chem. **99**, 2878 (1995).
- ¹⁴ E. Spohr, J. Chem. Phys. **106**, 388 (1997).
- ¹⁵ A. K. Soper, J. Phys. Condensed Matt. **9**, 2399 (1997).
- ¹⁶ Information on Vycor glass industrial preparation is available from Corning OEM Sales Service, Box 5000, Corning, New York 14830.
- ¹⁷ A. Brodka, and T. W. Zerda, J. Chem. Phys. **104**, 6319 (1996).
- ¹⁸ B. P. Feuston and S. H. Garofalini, J. Chem. Phys. **89** 5818 (1988).
- ¹⁹ R. W. G. Wyckoff, *Crystal structures*, 2nd ed. (Wiley, New York, 1963).
- ²⁰ A. Brodka and T. W. Zerda, J. Chem. Phys. **95**, 3710 (1991).
- ²¹ W. L. Jorgensen, J. Chandrasekhar, J. D. Madura, R. W. Impey, and M. L. Klein, J. Chem. Phys. **79**, 926 (1983).
- ²² M. P. Allen and D. J. Tildesley, *Computer Simulation of Liquids* (Oxford 1987).
- ²³ M. Neumann, J. Chem. Phys. **85**, 1567 (1986).
- ²⁴ M. J. Benham, J. K. Cook, J. C. Li, D. K. Ross, P. L. Hall, and B. Sarkissian, Phys. Rev. **B39**, 633 (1989).
- ²⁵ S. Iarlori, F. Ercolessi and E. Tosatti, in *Supercomputing tools for science and engineering*, ed. by D. Laforenza and R. Perego (Milan 1990), p. 463.
- ²⁶ B.M. Ladanyi and M. S. Skaf, Annu. Rev. Phys. Chem. **44**, 335 (1993).
- ²⁷ O. Glatter and O. Kratky, *Small angle X-ray scattering* (Academic Press, New York, 1992).
- ²⁸ J. P. Brodholt, F. Bruni, P. Jedlovsky, M. A. Ricci, A. K. Soper and R. Vallauri, J. Chem. Phys., in press.

TABLE I. Interaction potential parameters and fractional charges for water (TIP4P model) and silica sites; the locations of water sites in the molecular frame are also given

	Site	σ (\AA)	ϵ/k_B (K)	q e	x (\AA)	y (\AA)	z (\AA)
water ^a	O	3.154	78.0	0.0	0.0	-0.06556	0.0
	H	0.0	0.0	0.52	0.75695	0.52032	0.0
	H	0.0	0.0	0.52	-0.75695	0.52032	0.0
	X	0.0	0.0	-1.04	0.0	0.0844	0.0
silica ^b	Si	0.0	0.0	1.283			
	bO	2.70	230.0	-0.629			
	nbO	3.00	230.0	-0.533			
	Hs	0.0	0.0	0.206			

^aTIP4P model²¹. Label X here stands for the additional charge site of TIP4P model.

^bValues from Ref. 17; bO: bridging oxygens; nbO: non bridging oxygens; Hs: protons on the substrate surface.

Figure captions

Figure 1 - Computer simulated site-site distribution functions, calculated according to Eq. 1. Solid line represents distribution functions obtained by considering water confined in a interacting silica cavity; dashed line represents distribution functions of water confined in the same cavity but without any interaction with the substrate atoms. **a)** Oxygen-oxygen distribution function. **b)** Oxygen-hydrogen distribution function. **c)** Hydrogen-hydrogen distribution function.

Figure 2 - Computer simulated distribution functions, calculated according to Eq. (2), for confined water (solid lines). These functions have been corrected taking into account excluded volume effects, as explained in the text, and are compared with results obtained for bulk TIP4P water (dashed lines). Due to the approximations involved in the derivation (see text) the corrected functions are not reliable below the minimum approach distances, indicated by the arrow. **a)** Oxygen-oxygen distribution function. **b)** Oxygen-hydrogen distribution function. **c)** Hydrogen-hydrogen distribution function.

Figure 3a - Computer simulated distribution function of the substrate hydrogens (H_S) with respect to water oxygens (O_W).

Figure 3b - Computer simulated distribution function of the substrate oxygens (O_S) with respect to water hydrogens (H_W) (dashed line), and to water oxygens (O_W) (solid line).

Figure 4 - Layer analysis of the density profile of confined water as a function of distance from the center of the pore, calculated with the substrate-water interaction turned on (solid line) and off (dashed line).

Figure 5 - Layer analysis of the number of hydrogen bonds (n_{HB}) as a function of distance from the center of the pore, calculated with the substrate-water interaction turned on (solid line) and off (dashed line). The horizontal dotted line represents the density-weighted average value of n_{HB} for confined water with the substrate-water interaction turned on.

Figure 6a - Distributions of hydrogen bonds per molecule in layers 1, 5, and 9.

Figure 6b - Distributions of $\cos(\gamma)$, γ being the $H - O \cdots O$ angle between two H-bonded molecules, in layers 1, 5, and 9.

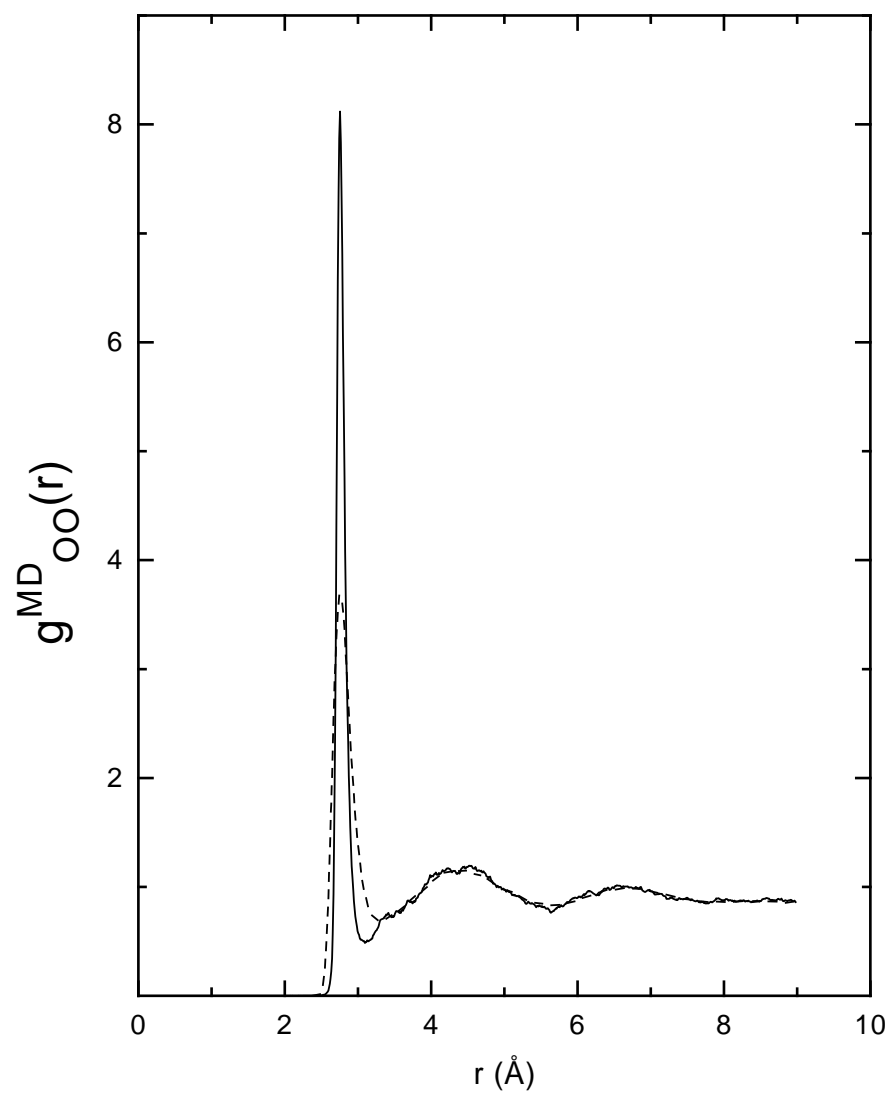


Fig. 1a

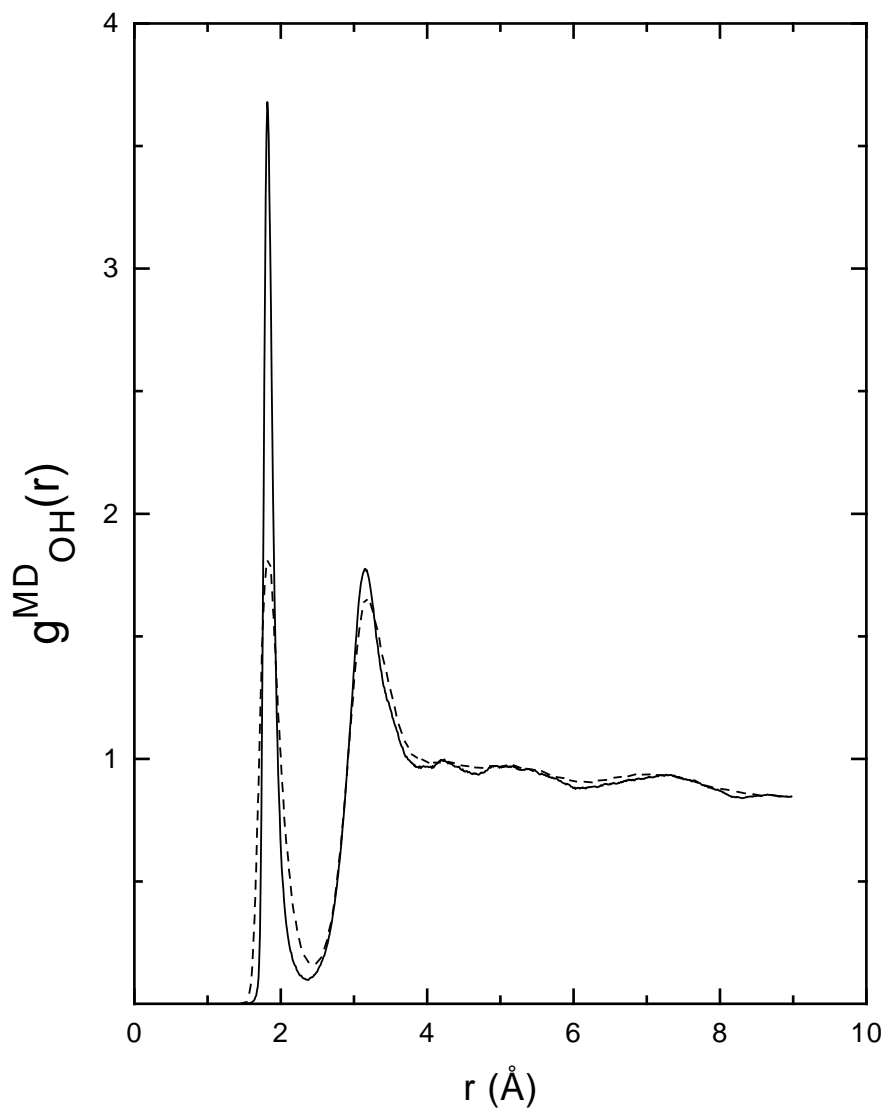


Fig. 1b

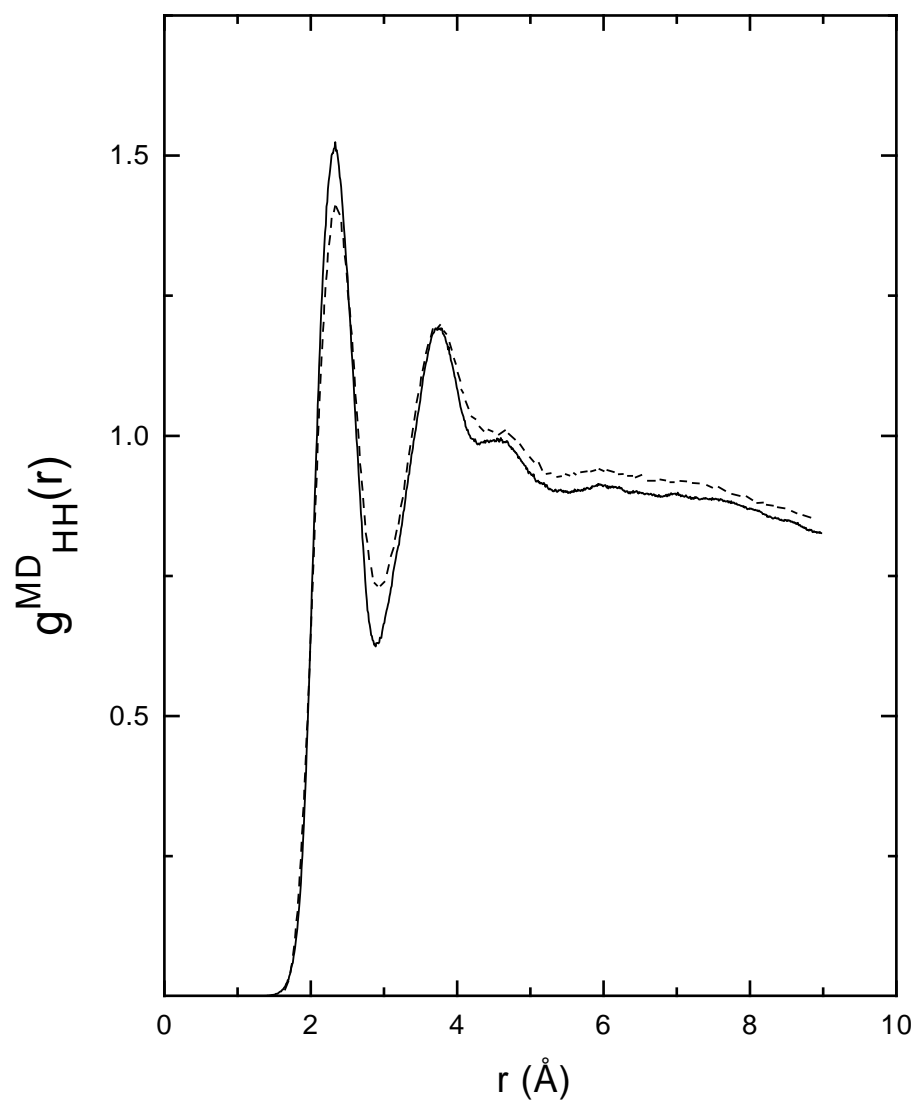


Fig. 1c

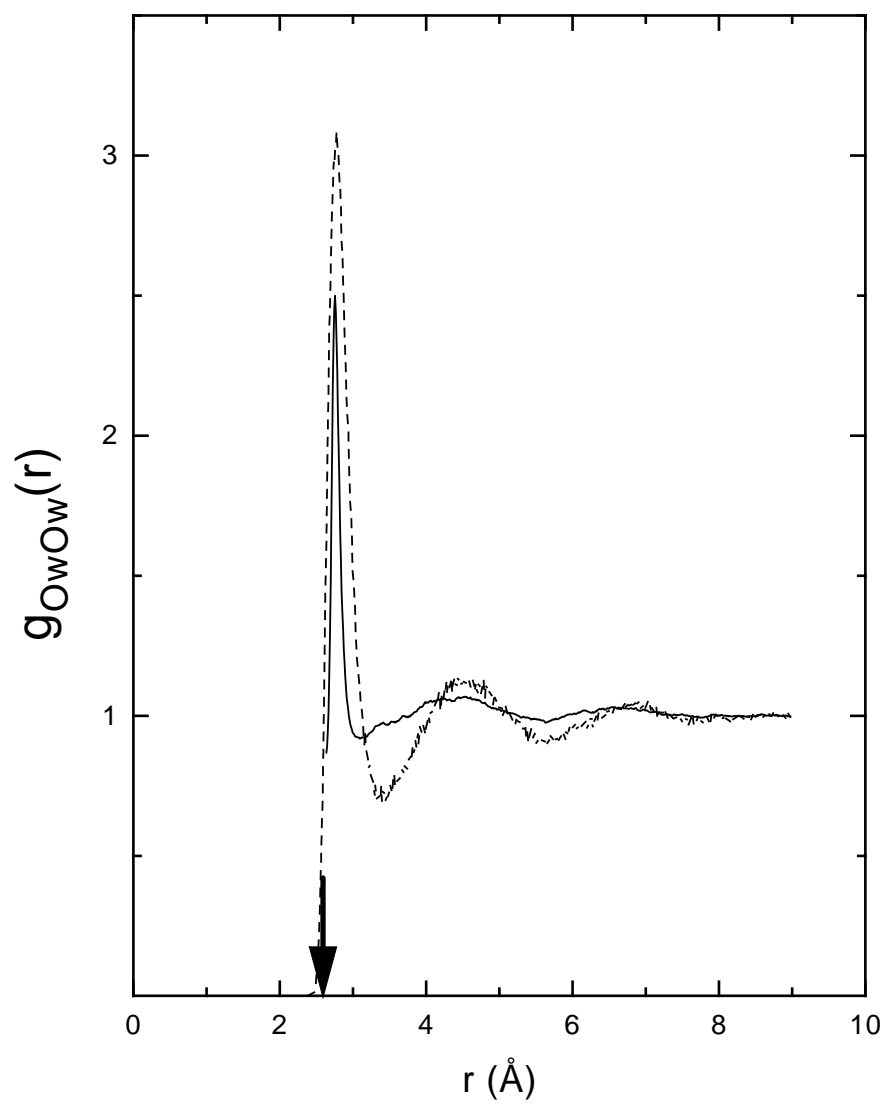


Fig. 2a

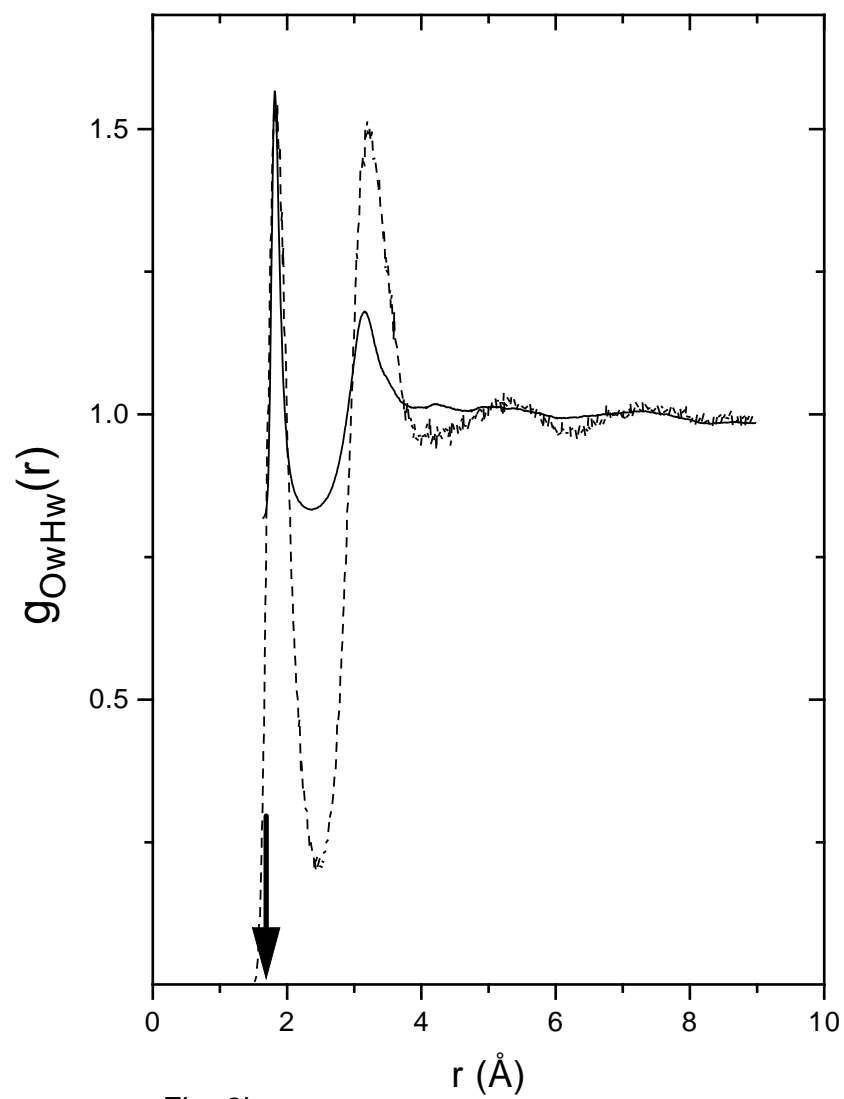
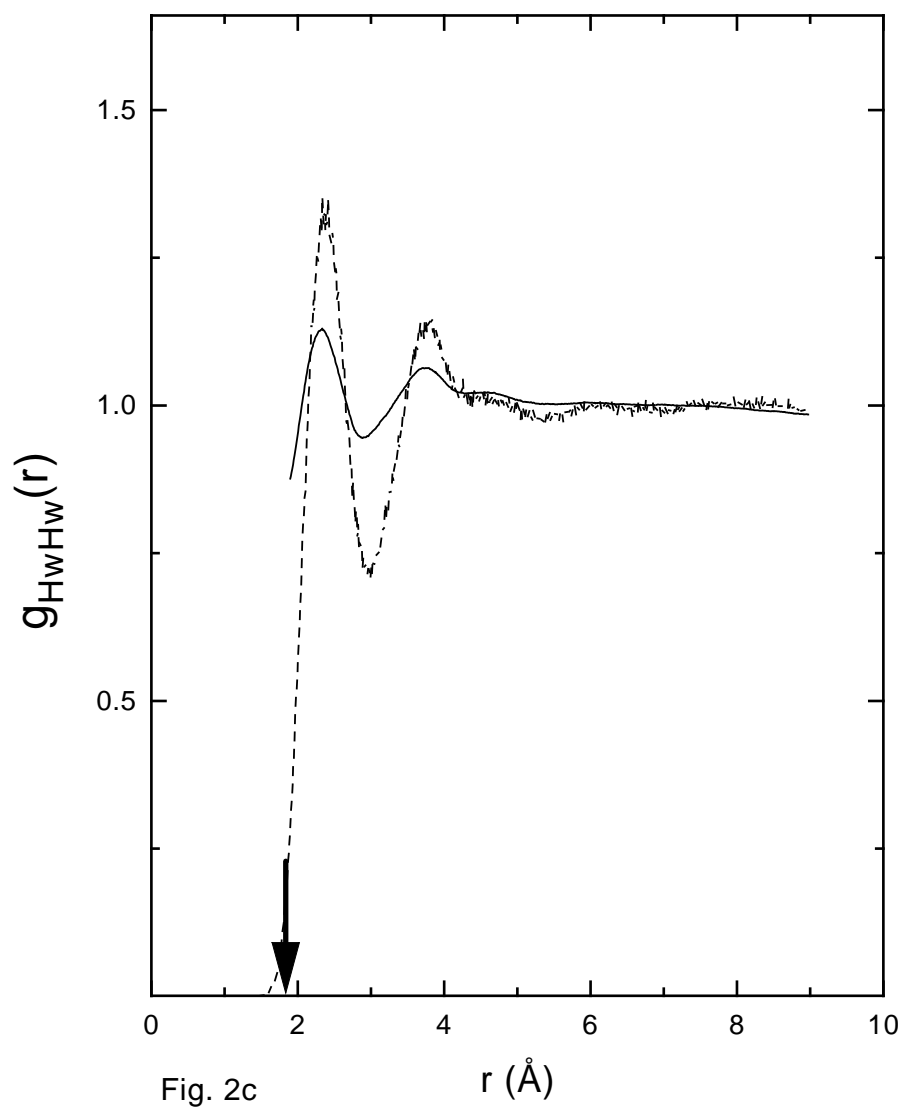


Fig. 2b



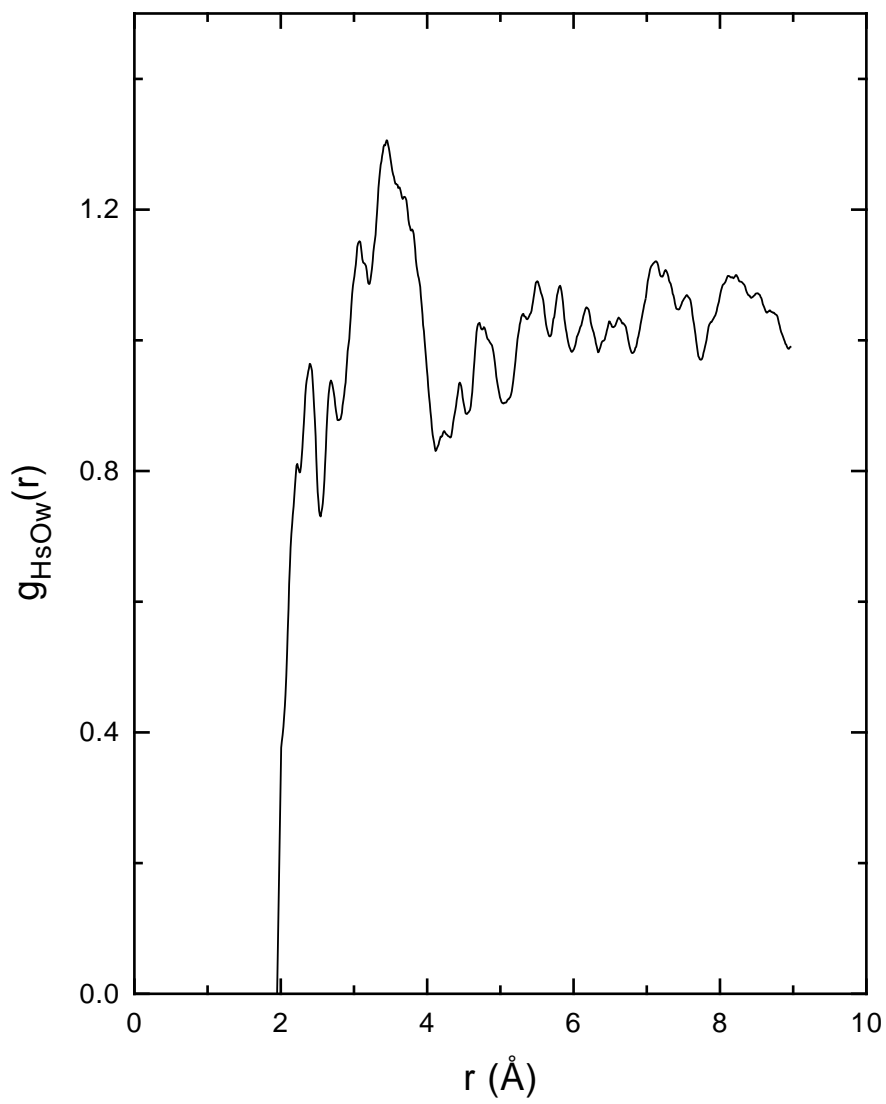


Fig. 3a

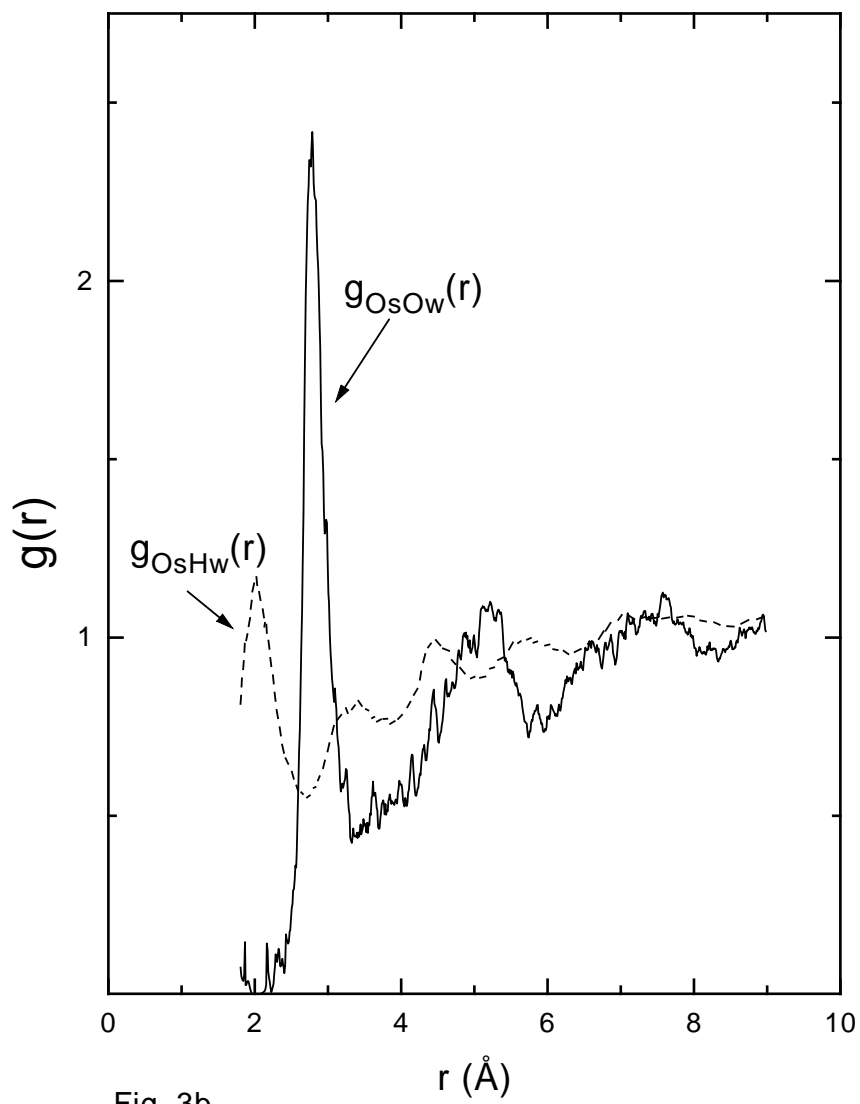


Fig. 3b

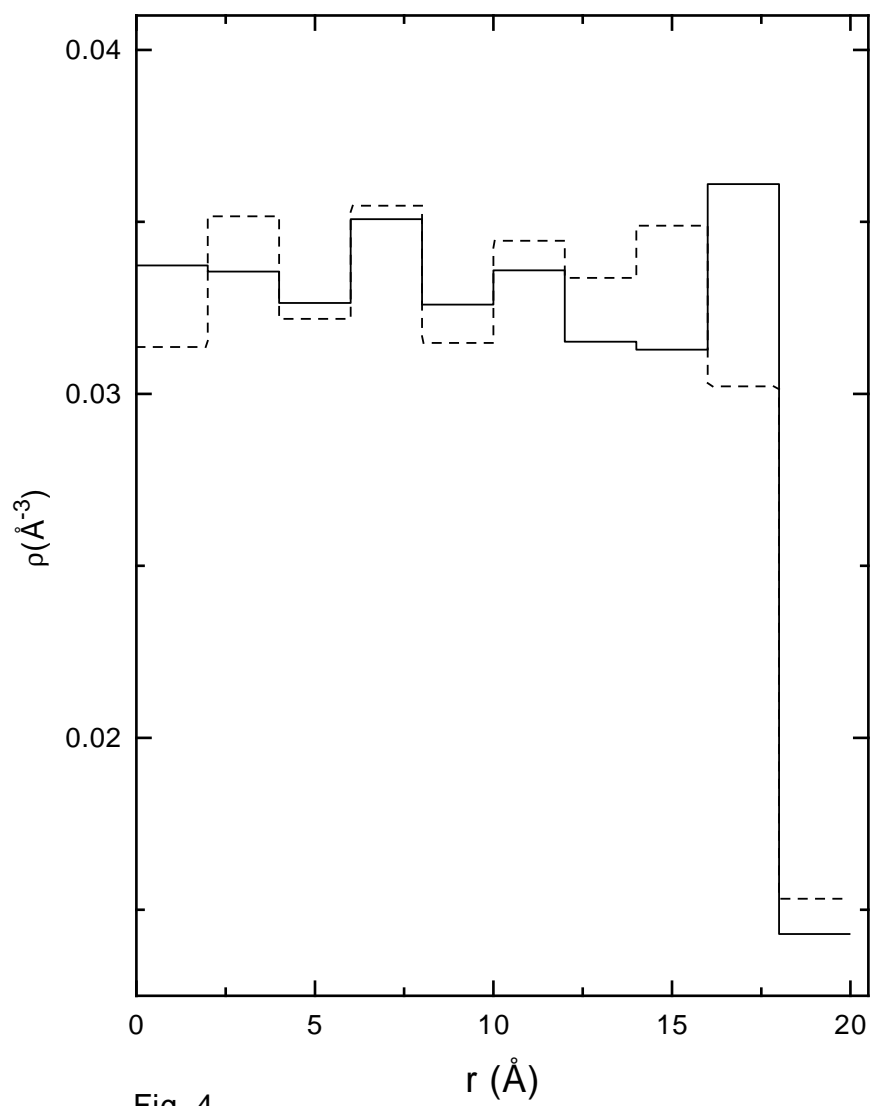


Fig. 4

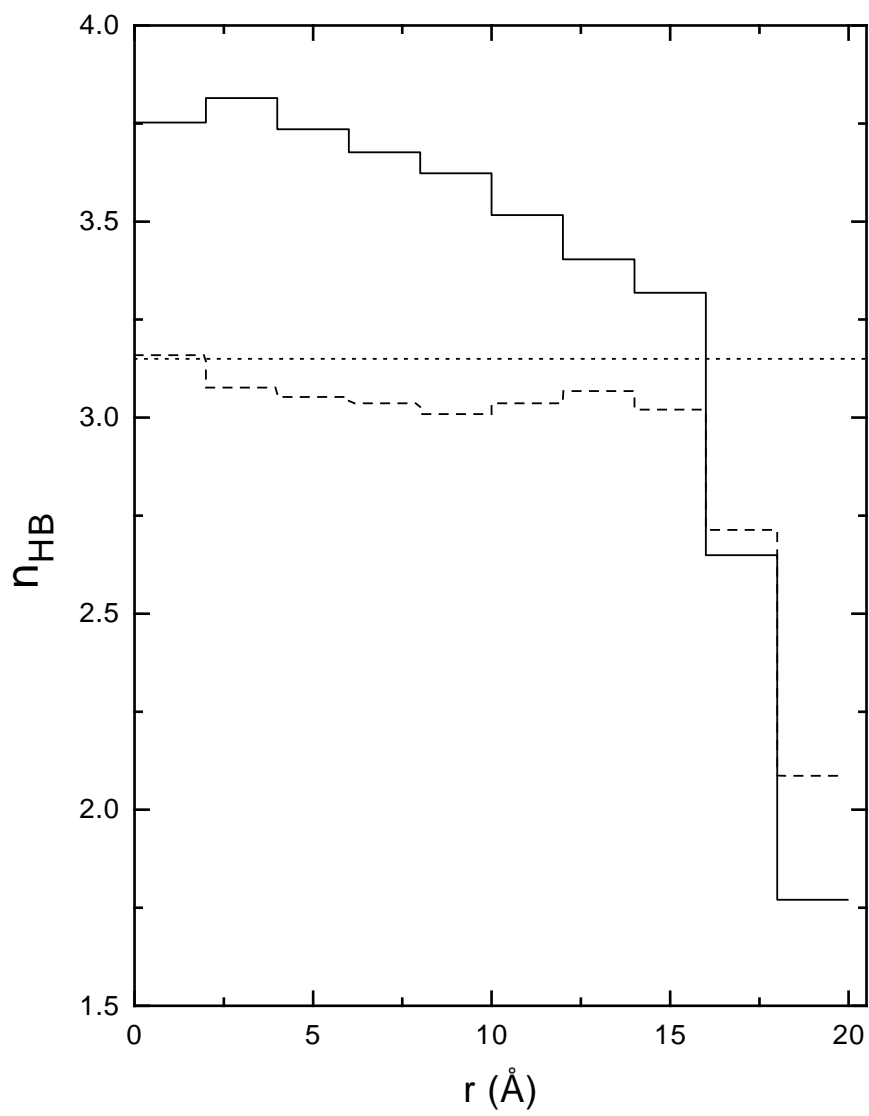
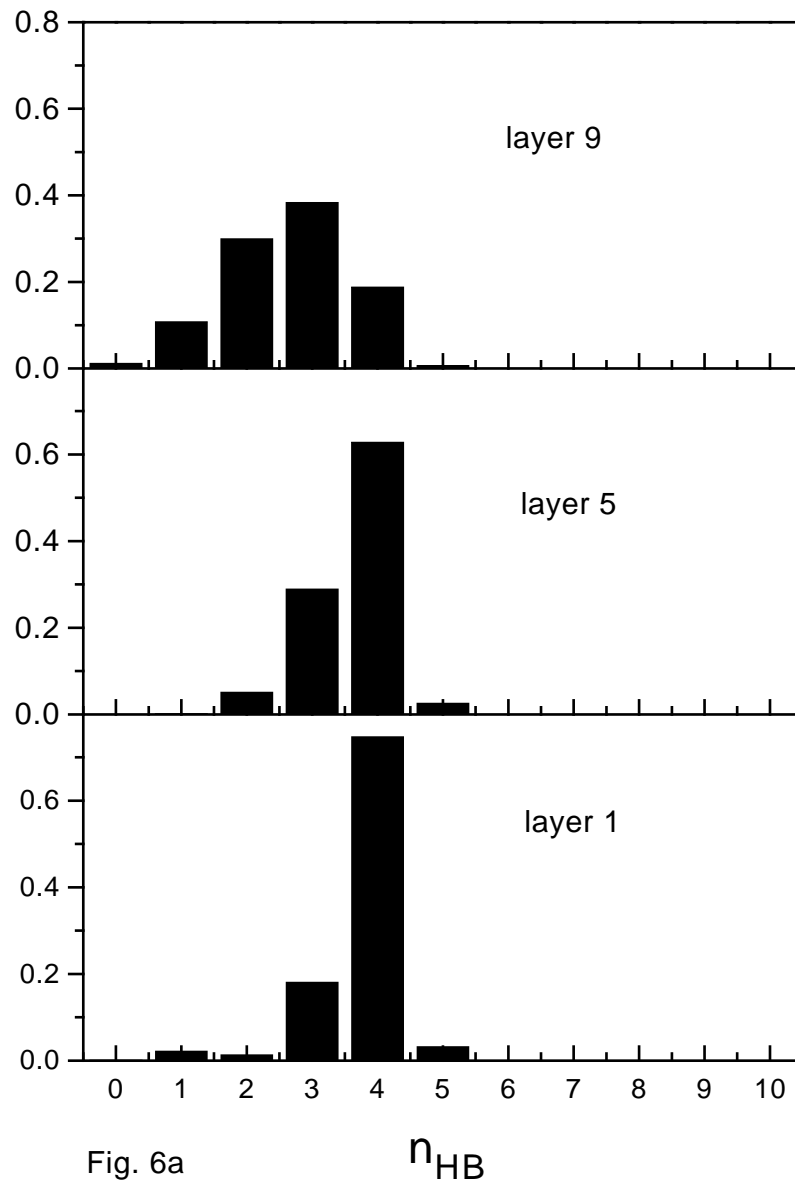


Fig. 5



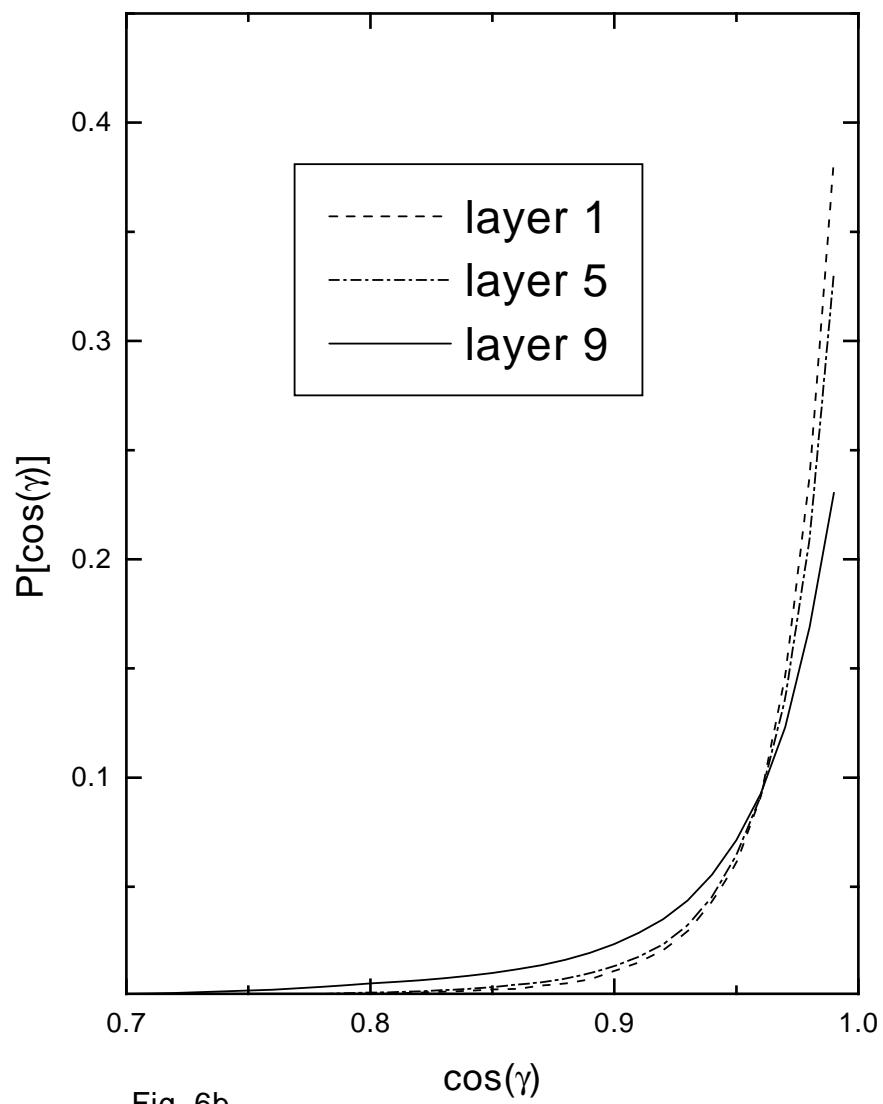


Fig. 6b